

## Comparison of Electrochemical Properties for Lithium-rich Cathode Material $\text{Li}[\text{Li}_{0.2}\text{Mn}_{0.54}\text{Ni}_{0.13}\text{Co}_{0.13}]\text{O}_2$ Prepared by Two Methods

Puheng Yang, Shichao Zhang\*, Xin Wei, Juan Meng, Yalan Xing

School of Materials Science and Engineering, Beihang University, Beijing 100191,

\*E-mail: [csc@buaa.edu.cn](mailto:csc@buaa.edu.cn)

Received: 17 June 2015 / Accepted: 19 August 2015 / Published: 30 September 2015

---

$\text{Li}[\text{Li}_{0.2}\text{Mn}_{0.54}\text{Ni}_{0.13}\text{Co}_{0.13}]\text{O}_2$  materials for lithium-ion battery have been successfully synthesized by gel-combustion (GC) and sol-gel (SG) methods. The as-prepared materials were characterized by XRD, SEM and electrochemical measurements. The XRD patterns show that the  $\text{Li}[\text{Li}_{0.2}\text{Mn}_{0.54}\text{Ni}_{0.13}\text{Co}_{0.13}]\text{O}_2$  materials obtained from different methods both form a pure phase with well crystallization. SEM images present that  $\text{Li}[\text{Li}_{0.2}\text{Mn}_{0.54}\text{Ni}_{0.13}\text{Co}_{0.13}]\text{O}_2$  obtained from gel-combustion method (GC-material) exhibited the relatively uniform distribution in particle size. The results of electrochemical measurements indicate that the GC-material showed the higher discharge capacity at 0.1C and lower solid electrolyte interface resistance and charge transfer resistance, while, the cycling stability of GC-material tested at 0.1C is relatively poor as compared to that of  $\text{Li}[\text{Li}_{0.2}\text{Mn}_{0.54}\text{Ni}_{0.13}\text{Co}_{0.13}]\text{O}_2$  obtained from sol-gel method (SG-material).

---

**Keywords:** Li-ion battery; Li-rich material; Sol-gel; Gel-combustion

### 1. INTRODUCTION

Rechargeable lithium ion batteries account for the majority of portable electronic devices market. They are also considered as serious candidates to promote the development of electric vehicles as well as the field of intermittent renewable energy sources. To satisfy the demand of hybrid electric vehicle (HEV) and electric vehicle (EV), cathode materials with higher energy density, lower cost, higher voltage and more safety features are desired. Compared with commercialized cathode materials, such as conventional layered  $\text{LiCoO}_2$ ,  $\text{Li}[\text{Mn}_{1/3}\text{Ni}_{1/3}\text{Co}_{1/3}]\text{O}_2$ , olivine  $\text{LiFePO}_4$ , and spinel  $\text{LiMn}_2\text{O}_4$ , lithium-rich layered oxides deliver much higher specific capacity (over 250 mAh/g) with operating potentials higher than 3.5 V (vs.  $\text{Li/Li}^+$ ) in average.[1] Electrode structure stabilization and

enhancement of discharge capacity by extracting the lithium accompanying oxygen (a net loss of  $\text{Li}_2\text{O}$ ) at 4.5-4.8V of the  $\text{Li}_2\text{MnO}_3$  component in lithium-rich cathode materials have been investigated extensively.[2-4] During the first charge above 4.5V (vs.  $\text{Li}/\text{Li}^+$ ), partial capacity of the materials results from an activation process accompanied by irreversible oxygen loss from the lattice of  $\text{Li}_2\text{MnO}_3$ , which causes the oxidation state of the transition metal ions after the first cycle lower than that of the initial materials.[5, 6] Among the promising Lithium-rich materials ( $x\text{Li}_2\text{MnO}_3 \cdot (1-x)\text{LiNi}_{1/3}\text{Co}_{1/3}\text{Mn}_{1/3}\text{O}_2$ ),  $\text{Li}[\text{Li}_{0.2}\text{Mn}_{0.54}\text{Ni}_{0.13}\text{Co}_{0.13}]\text{O}_2$  could deliver notable high capacity up to  $300 \text{ mAh g}^{-1}$  with good cycling performance.[3, 7]

Despite remarkable capacity lithium-rich materials demonstrate, series of drawbacks make them far from commercial application, such as safety problems resulting from release of nominal " $\text{Li}_2\text{O}$ " during the first cycle,[6] low rate capability caused by insulating  $\text{Li}[\text{Li}_{1/3}\text{Mn}_{2/3}]\text{O}_2$  component,[8] and high operating voltage leading to thick solid-electrolyte interfacial.[9]

A number of research groups have recently paid attention to improve the electrochemical performance of  $\text{Li}[\text{Li}_{0.2}\text{Mn}_{0.54}\text{Ni}_{0.13}\text{Co}_{0.13}]\text{O}_2$ . Traditional methods have been adopted to synthesize lithium-rich materials, such as co-precipitation,[1, 10] sol-gel,[9] sucrose combustion,[11] and radio frequency magnetron sputtering method.[12] However, compounds formed via these ways can result in micron aggregates, and thus impede Li-ion transport as well as cause inhomogeneous mixture.[13, 14] Gel-combustion is an available way to reduce scale of the particles and uniform the mixture.[15] And to the best of our knowledge, there was the first time gel-combustion method applied on the synthesis and electrochemical performance of  $\text{Li}[\text{Li}_{0.2}\text{Mn}_{0.54}\text{Ni}_{0.13}\text{Co}_{0.13}]\text{O}_2$ .

In this work, gel-combustion (GC) method and sol-gel(SG) method, two different synthesis methods of  $\text{Li}[\text{Li}_{0.2}\text{Mn}_{0.54}\text{Ni}_{0.13}\text{Co}_{0.13}]\text{O}_2$ , were studied and compared thoroughly to understand effect on structure, morphology and electrochemical performance of  $\text{Li}[\text{Li}_{0.2}\text{Mn}_{0.54}\text{Ni}_{0.13}\text{Co}_{0.13}]\text{O}_2$ . It is believed that the comparison of distinct methods should be instrumental to understand the advantage and disadvantage clearly, and thus come up with a more suitable method to synthesize the promising lithium-rich cathode material.

## 2. EXPERIMENTAL

$\text{Li}[\text{Li}_{0.2}\text{Mn}_{0.54}\text{Ni}_{0.13}\text{Co}_{0.13}]\text{O}_2$  materials were prepared by two different preparation methods, gel-combustion (GC) and sol-gel (SG) methods. All the chemicals used are AR grade.

### 2.1 Gel-combustion (GC) method

$\text{Li}[\text{Li}_{0.2}\text{Mn}_{0.54}\text{Ni}_{0.13}\text{Co}_{0.13}]\text{O}_2$  composite was synthesized via a mannitol assisted gel-combustion method. A stoichiometric amount of nickel acetate, cobalt acetate, manganese acetate and lithium acetate were dissolved in 40 mL deionized water, subsequently, mannitol solution was added dropwise into the metal acetate solution as complexing and burning agent under continually stirring. Dilute nitric acid was applied to adjust the pH of the mixed solution, and then the transparent sol was dried at  $80^\circ\text{C}$  under magnetic stirring and heated up to burn spontaneously to form black ash. Finally, the ash was

sintered at 900 °C for 15 h to obtain the target compound. The as-prepared sample synthesized by gel-combustion method is indicated as GC-material.

## 2.2 Sol-gel (SG) method

Li[Li<sub>0.2</sub>Mn<sub>0.54</sub>Ni<sub>0.13</sub>Co<sub>0.13</sub>]O<sub>2</sub> composite was synthesized via a citric acid assisted sol-gel method. A stoichiometric amount of nickel nitric, cobalt nitric, manganese nitric and lithium nitric were dissolved into deionized water. Then citric acid solution acting was added dropwise into the metal nitric solution as chelating agent under magnetic stirring. The solution was heated at 80 °C with continuous stirring until a transparent sol and then gel was obtained. The dried precursor was precalcined at 350 °C for 2 h with consequently calcining at 900 °C for 15 h. The as-prepared sample synthesized by sol-gel method is indicated as SG-material.

## 2.3 Materials characterization

X-ray diffraction (XRD, Rigaku D/Max-2400, Japan) with Cu K $\alpha$  radiation was applied to identify the crystalline structure of as-prepared materials. The XRD spectra were detected with  $2\theta$  value ranging from 10° to 80°. Scanning electron microscopy (SEM, Hitachi S-4800, Japan) concomitant with energy-dispersive X-ray spectroscopy (EDX) were used to observe morphology, size distribution and element proportion of the synthesized material.

## 2.4 Electrochemical measurements

Electrochemical measurements were carried out using CR2025 coin-type cells. The cathodes were prepared by coating a mixture of 80% active material, 10% acetylene black, 10% PVDF binder on circular Al current collector foils with diameter of 1cm. The electrodes were then dried in a vacuum oven at 100°C for 2 h. The testing half-cells were assembled in an argon-filled glove box (MB-10-G with TP170b/mono, MBRAUN) with lithium metal as counter and reference electrode. Electrolyte was 1 M LiPF<sub>6</sub> in a mixed solution of EC, DEC and DMC (1:1:1 in volume ratio). The charge–discharge measurements were galvanostatically carried out by using a battery test system (NWEARE BTS-610, Neware Technology Co., Ltd., China). All the batteries were tested at the voltage range between 2.0 V and 4.8 V vs. Li/Li<sup>+</sup> with current density of 25mA g<sup>-1</sup> at room temperature. The cyclic voltammograms (CV) were measured by using an electrochemical station (CHI660a) at a scanning rate of 0.1 mV s<sup>-1</sup> with the voltage ranging from 2.0 V to 4.8 V.

# 3. RESULTS AND DISCUSSION

## 3.1 XRD structural characterization

XRD patterns of Li[Li<sub>0.2</sub>Mn<sub>0.54</sub>Ni<sub>0.13</sub>Co<sub>0.13</sub>]O<sub>2</sub> synthesized by sol-gel and gel-combustion method are shown in Fig.1. All the diffraction peaks can be indexed as layered lattice based on the  $\alpha$ -

NaFeO<sub>2</sub> structure with space group *R-3m* except the weak peaks between 20° and 25° identified as the (020) reflection of the super lattice structure of the Li<sub>2</sub>MnO<sub>3</sub>-like component (*C2/m* space group).[16-18] The lattice parameters of the samples based on the *R-3m* structure calculated by Rietveld refinements are listed in table 1. Both materials show high lattice parameter ratios of *c/a* (higher than 4.98), value of  $I_{(003)}/I_{(104)}$  (larger than 1.2) and well split (006)/(102) and (108)/(110) peaks, indicating pure phase with good crystallinity formed without undesirable cation mixing.[19] Compared with SG-material, GC-material exhibits higher value of  $I_{(003)}/I_{(104)}$ , suggesting GC-material shows the better the cation order.

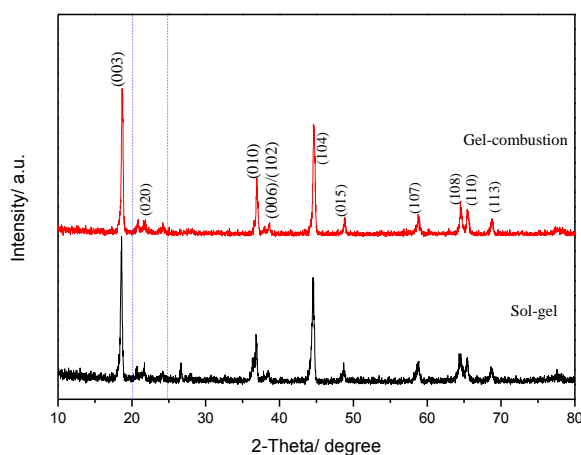


**Figure 1.** XRD patterns of as-prepared cathode materials

**Table 1.** The crystal structure parameters and of prepared powders, calculated by Rietveld refinements

Method	a (Å)	c (Å)	<i>c/a</i>	$I_{(003)}/I_{(104)}$	Volume (Å <sup>3</sup> )
Sol-gel	2.847	14.219	4.995	1.320	99.8
Gel-combustion	2.852	14.220	4.986	1.384	100.2

### 3.2 Morphology characterization

SEM images of Li[Li<sub>0.2</sub>Mn<sub>0.54</sub>Ni<sub>0.13</sub>Co<sub>0.13</sub>]O<sub>2</sub> synthesized by sol-gel and gel-combustion methods are shown in Fig.2 with different magnifications. The SEM images reveal that both materials are aggregated from submicron particles. It can be seen from Fig.2a and Fig.2c that the particle size of SG-material (100-400 nm) is less homogeneous than that of the GC-material (around 300 nm). It can be indicated from the lower magnification images that particle aggregation in the GC-material is lighter than SG-material, and it is in good agreement with the previous report.[15]

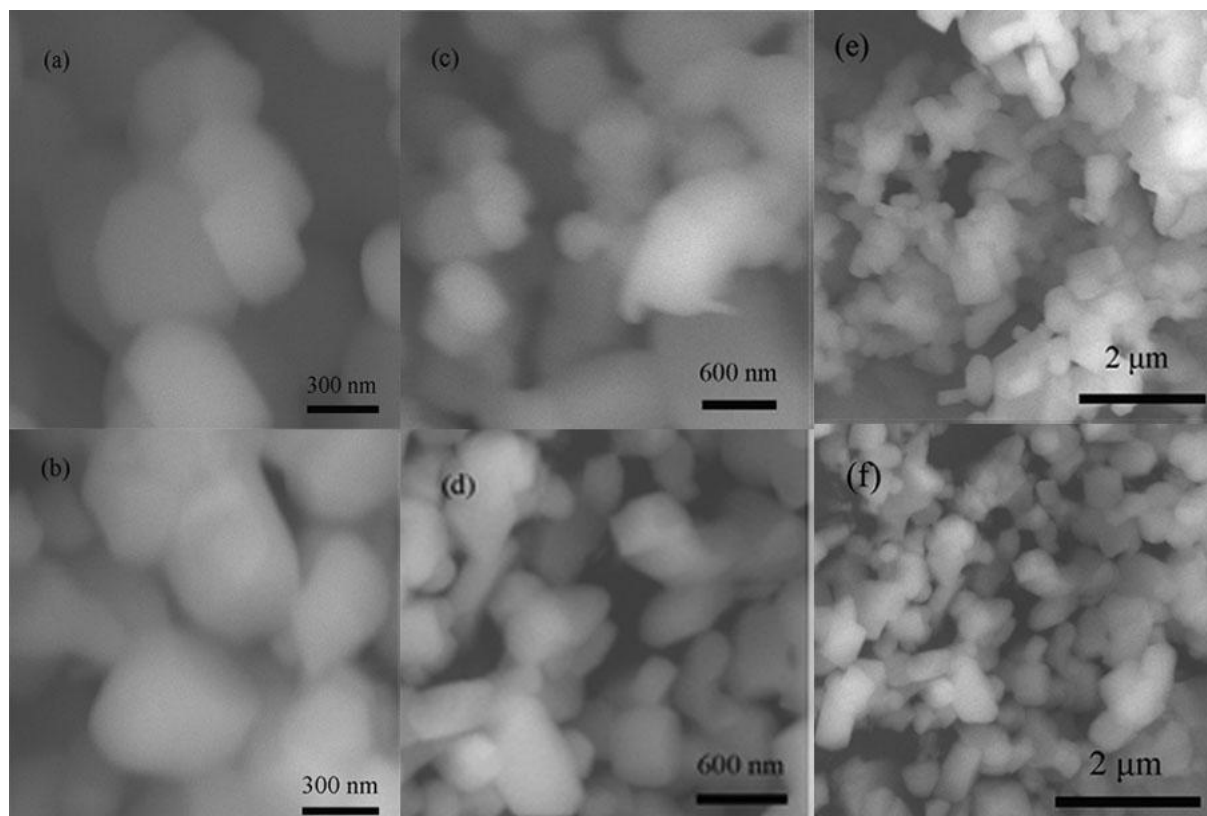
**Table 2.** The EDX results of  $\text{Li}[\text{Li}_{0.2}\text{Mn}_{0.54}\text{Ni}_{0.13}\text{Co}_{0.13}]\text{O}_2$  materials synthesized by sol-gel method and gel-combustion method

Method	Mn (at %)	Co (at %)	Ni (at %)	O (at %)
Sol-gel	15.82	4.23	3.74	76.21
Gel-combustion	15.71	4.44	3.97	75.88

The EDX results were listed in table 2, despite O values overestimated as we reported previously,[20] the atomic ratios of both materials are close to the stoichiometric ratios of raw materials.

### 3.3 Electrochemical properties of SG- material and GC-material

The cycle performance of  $\text{Li}[\text{Li}_{0.2}\text{Mn}_{0.54}\text{Ni}_{0.13}\text{Co}_{0.13}]\text{O}_2$  synthesized by sol-gel method and gel-combustion method cycled at 0.1C in the voltage range of 2.0-4.8 V are revealed in Fig.3. As can be seen in Fig.3a, the GC-material delivers the higher initial discharge capacity ( $238\text{mAh g}^{-1}$ ) than SG-material ( $202\text{mAh g}^{-1}$ ).

**Figure 2.** Scanning electron microscopy images of  $\text{Li}[\text{Li}_{0.2}\text{Mn}_{0.54}\text{Ni}_{0.13}\text{Co}_{0.13}]\text{O}_2$  materials synthesized by (a, c and e) sol-gel method and (b, d and f) gel-combustion method

In the following cycles, the capacity losses of both materials are relatively high before the first

5 cycles compared with the subsequent cycles for GC-material, it may be caused by the continuous "Li<sub>2</sub>O" loss during the several initial cycles. At the end of 15th cycle, SG-material and GC-material retains discharge capacities of 191 and 215 mAh g<sup>-1</sup>, and their corresponding capacity retention ratios relative to the highest capacity among 15 cycles are 94.5% and 90.3%, respectively. The result indicates that although GC-material reveals the higher discharge capacity, the cycling performance of SG-material is relatively superior at 0.1C. Fig. 3b and Fig. 3c depict the charge and discharge curves between 2.0 and 4.8V for GC-material and SG-material in different cycles at 0.1C, respectively. During the first cycle, the charge curve mainly comprises of two regions corresponding to different electrochemical reactions for both materials. The first sloping region can be attributed to transition metal oxidation reaction (Ni<sup>2+</sup> → Ni<sup>4+</sup> and Co<sup>3+</sup> → Co<sup>3.6+</sup>), [21, 22] while the subsequent plateau region is assigned to the irreversible removal of Li<sub>2</sub>O from the electrode. [15, 23] The length of sloping region and plateau region of GC-material are both longer than SG-material, indicating that GC-material has the better transition metal oxidation reaction and Li<sub>2</sub>MnO<sub>3</sub> component activation. The curve for first discharge process shows that the GC-material has the relatively high initial capacity compared to SG-material, agreed with Fig.3a well. During the subsequent cycles, the plateau regions disappear in the charge curves for both materials, accounting for the complement of irreversible Li<sub>2</sub>O release during the first several cycles. Both materials can be modified by doping cation ions and coating electrochemical inert compounds, and these two methods are proved to be available to enhance the performance of other cathode materials. [24, 25]

The electrochemical properties further studied by cyclic voltammetric method at a scan rate of 0.1 mV s<sup>-1</sup> are shown in Fig.4. There are two anodic peaks during the initial charge process for both materials (named as peak a<sub>1</sub> and a<sub>2</sub>), peak a<sub>1</sub> can be attributed to transition metal oxidation reaction (Ni<sup>2+</sup> → Ni<sup>4+</sup> and Co<sup>3+</sup> → Co<sup>3.6+</sup>), while peak a<sub>2</sub> corresponds to oxygen loss with Li extraction, consistent with the first charge curves in Fig.3b and Fig.3c. The corresponding cathodic peaks of Ni<sup>4+</sup> to Ni<sup>2+</sup> and Co<sup>3.6+</sup> to Co<sup>2+</sup> are also observed during the initial discharge process, named as peak c<sub>1</sub> and c<sub>2</sub>, respectively, while the cathodic peak of Mn ions due to the loss of oxygen is named as peak c<sub>3</sub>. In the subsequent cycles, the CV curves are significantly different from the first cycle. During the charge process, peak a<sub>2</sub> disappears and peak a<sub>1</sub> shifts to lower voltage gradually, indicating that the process of oxygen releasing has already completed and the bulk structure and/or the electrode surface area of the materials may have been modified after the first cycle. The voltage gaps between the anodic and cathodic peaks of SG-material are smaller than those of GC-material, demonstrating that the reversibility of the SG-material is better than the GC-material.

The difference in interfacial electrochemistry and reaction kinetics for Li[Li<sub>0.2</sub>Mn<sub>0.54</sub>Ni<sub>0.13</sub>Co<sub>0.13</sub>]O<sub>2</sub> prepared by sol-gel and gel-combustion methods has been studied by electrochemical impedance spectroscopy. The measurements were carried out in the charge state of 4.8V at the initial cycle. Fig. 5 shows the Nyquist plots of Li[Li<sub>0.2</sub>Mn<sub>0.54</sub>Ni<sub>0.13</sub>Co<sub>0.13</sub>]O<sub>2</sub> electrode tested from 100 kHz to 10 mHz, in which Z<sub>im</sub> and Z<sub>re</sub> denote the imaginary and real part of impedances, respectively. And the inset one in Fig. 4 is the equivalent circuit employed for fitting the EIS spectra. A high-frequency semicircle, an inter-mediate-frequency semicircle and a low-frequency tail in the Nyquist plots are related to the solid electrolyte interface resistance (R<sub>SEI</sub>), charge transfer process resistance (R<sub>ct</sub>) of the electrode/ electrolyte interface and Li<sup>+</sup> ion diffusion process in the solid phase of

electrode, respectively. The fitted results of  $R_{SEI}$  and  $R_{ct}$  values are listed in Table 3. Compared to  $R_{SEI}$  value,  $R_{ct}$  value is relatively high, indicating that the electrochemical performance is mainly influenced by charge transfer process.

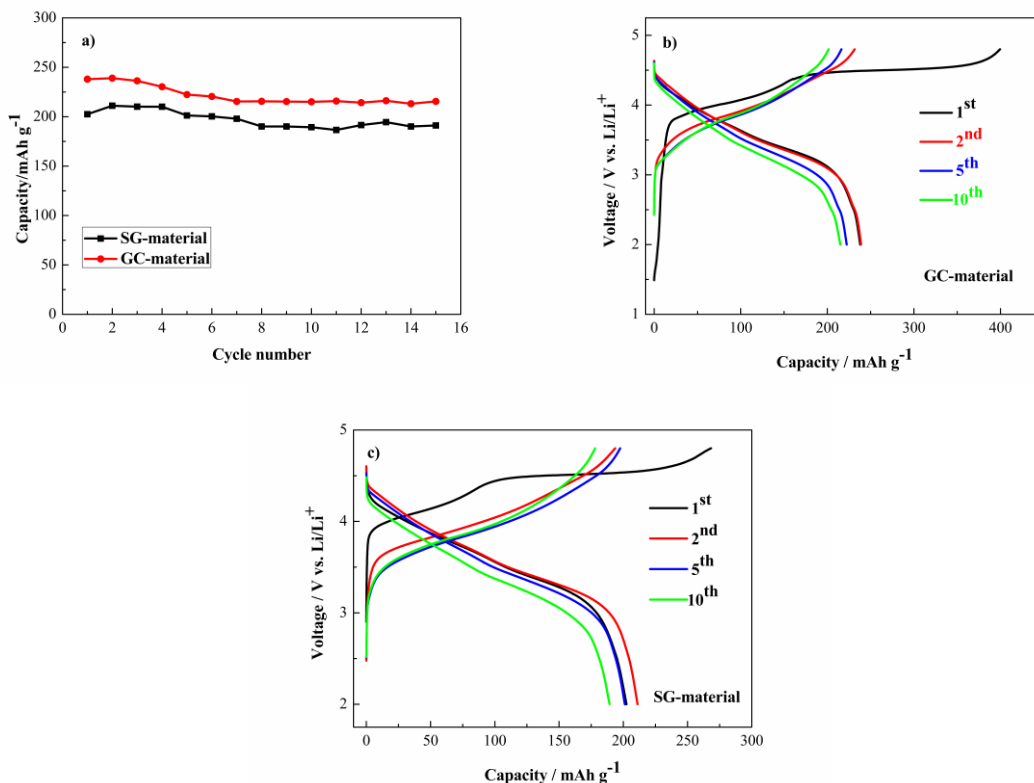


**Figure 3.** a) Cycling performance and the charge/discharge profiles of  $\text{Li}[\text{Li}_{0.2}\text{Mn}_{0.54}\text{Ni}_{0.13}\text{Co}_{0.13}]\text{O}_2$  prepared by b) gel- combustion method and c) sol-gel method at 0.1C

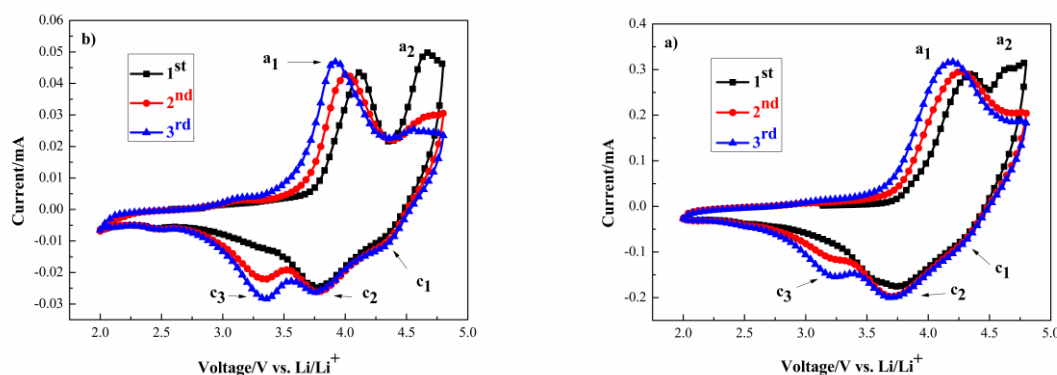


**Figure 4.** Cyclic voltammogram of  $\text{Li}[\text{Li}_{0.2}\text{Mn}_{0.54}\text{Ni}_{0.13}\text{Co}_{0.13}]\text{O}_2$  materials prepared by a) sol-gel method and b) gel-combustion method obtained at a scan rate of 0.1 mV/ s

$R_{SEI}$  of Li/GC-material cell is measured to 39.47  $\Omega$ , far more lower than that of Li/SG-material (154.5  $\Omega$ ), mainly resulting from the smaller particles providing larger surface area.[11] Thicker SEI

film caused by larger surface area also leads to higher  $R_{ct}$ . Lower  $R_{SEI}$  and  $R_{ct}$  values indicate that GC-material has the higher electronic conductivity, accounting for it having the relatively high capacity.

**Table 3.**  $R_{SEI}$  and  $R_{ct}$  values of  $\text{Li}[\text{Li}_{0.2}\text{Mn}_{0.54}\text{Ni}_{0.13}\text{Co}_{0.13}]\text{O}_2$  electrodes synthesized by sol-gel method and gel-combustion method at 4.8V

Method	$MR_{SEI}(\Omega)$	$R_{ct}(\Omega)$
Sol-gel	154.5	305.7
Gel-combustion	39.47	135.1

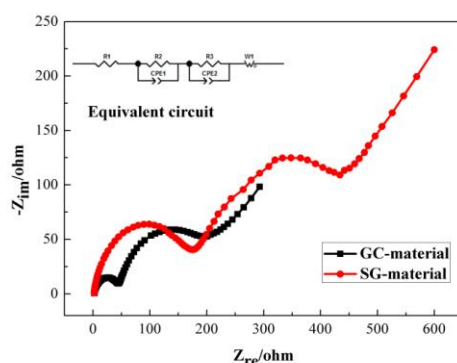


**Figure 5.** Nyquist plots of EIS spectra for Li/GC-material and SC-material cells charged to 4.8V

#### 4. CONCLUSIONS

The effects of different synthesis methods on structure, morphology and electrochemical performance of cathode materials  $0.5\text{Li}_2\text{MnO}_3 \cdot 0.5\text{LiMn}_{1/3}\text{Co}_{1/3}\text{Ni}_{1/3}\text{O}_2$  have been studied. Both materials are pure phase structured with good crystallinity. Although the SG-material has some smaller particles, the particle size distribution of GC-material is more uniform. Owing to better morphology characteristic, GC-material exhibits higher discharge capacity at 0.1 C as compared to SG-material. The uniform particle size of GC-material also leads to lower solid electrolyte interface resistance and charge transfer process resistance. In summary, the results suggest that the material synthesized by sol-gel method may be fitness for long-life lithium-ion battery, while the material synthesized by gel-combustion method is appropriate for lithium-ion battery that requires high capacity.

#### References

1. J.M. Zheng, D.R. Zhu, Y. Yang, Y.S. Fung, *Electrochim. Acta*, 59 (2012) 14.
2. M.M. Thackeray, C.S. Johnson, J.T. Vaughey, N. Li, S.A. Hackney, *J. Mater. Chem.*, 15 (2005) 2257.
3. C.S. Johnson, N. Li, C. Lefief, M.M. Thackeray, *Electrochem. Commun.*, 9 (2007) 787.

4. C.S. Johnson, J.S. Kim, C. Lefief, N. Li, J.T. Vaughey, M.M. Thackeray, *Electrochem. Commun.*, 6 (2004) 1085.
5. Z.H. Lu, J.R. Dahn, *J. Electrochem. Soc.*, 149 (2002) A815.
6. A.R. Armstrong, M. Holzapfel, P. Novak, C.S. Johnson, S.H. Kang, M.M. Thackeray, P.G. Bruce, *J. Am. Chem. Soc.*, 128 (2006) 8694.
7. Y. Wu, A.V. Murugan, A. Manthiram, *J. Electrochem. Soc.*, 155 (2008) A635.
8. M.M. Thackeray, S.H. Kang, C.S. Johnson, J.T. Vaughey, R. Benedek, S.A. Hackney, *J. Mater. Chem.*, 17 (2007) 3112.
9. J. Liu, A. Manthiram, *Chem. Mater.*, 21 (2009) 1695.
10. B.H. Song, Z.W. Liu, M.O. Lai, L. Lu, *Phys. Chem. Chem. Phys.*, 14 (2012) 12875.
11. J.M. Zheng, X.B. Wu, Y. Yang, *Electrochim. Acta*, 56 (2011) 3071.
12. H. Yim, W.Y. Kong, Y.C. Kim, S.J. Yoon, J.W. Choi, *J. Solid State Chem.*, 196 (2012) 288.
13. C.J. Jafta, K.I. Ozoemena, M.K. Mathe and W.D. Roos, *Electrochim. Acta*, 85 (2012) 411.
14. D. Luo, G. Li, X. Guan, C. Yu, J. Zheng, X. Zhang and L. Li, *J. Mater. Chem. A*, 1 (2013) 1220.
15. C.C. Fu, G.S. Li, D. Luo, J. Zheng and L.P. Li, *J. Mater. Chem. A*, 2 (2014) 1471.
16. J. Gao, A. Manthiram, *J. Power Sources*, 191 (2009) 644.
17. A.D. Robertson, P.G. Bruce, *Chem. Mater.* 15 (2003) 1984.
18. W.S. Yoon, S. Iannopollo, C.P. Grey, D. Carlier, J. Gorman, J. Reed, G. Ceder, *Electrochem. Solid State Lett.*, 7 (2004) A167.
19. Z.H. Lu, L.Y. Beaulieu, R.A. Donaberger, C.L. Thomas, J.R. Dahn, *J. Electrochem. Soc.*, 149 (2002) A778.
20. X. Wei, S.C. Zhang, Z.J. Du, P.H. Yang, J. Wang, Y.B. Ren, *Electrochim. Acta*, 107 (2013) 549.
21. T.A. Arinkumar, Y. Wu, A. Manthiram, *Chem. Mater.*, 19 (2007) 3067.
22. Y. J. Park, Y. S. Hong, X. Wu, M. G. Kim, K. S. Ryu, S. H. Chang, *J. Electrochem. Soc.*, 151 (2004) A720.
23. B.H. Song, M.O. Lai, L. Lu, *Electrochim. Acta*, 80 (2012) 187.
24. X.C. Sun, K. Sun, Y.Q. Wang, X.D. Bai, C.Y. Chen, B. Cui, *Int. J. Electrochem. Sci.*, 8 (2013) 12816.
25. H.L. Zhang, L. Zhang, S.W. Yang, *Int. J. Electrochem. Sci.*, 9 (2014) 8182.

© 2015 The Authors. Published by ESG ([www.electrochemsci.org](http://www.electrochemsci.org)). This article is an open access article distributed under the terms and conditions of the Creative Commons Attribution license (<http://creativecommons.org/licenses/by/4.0/>).